Indepth diagnosis of a secondary clarifier by the application of radiotracer technique and numerical modeling

H.S. Kim*, M.S. Shin*, D.S. Jang* and S.H. Jung**

*Department of Environmental Engineering, Chungnam National University, 220 Gungdong Yusunggu, Daejeon 305-764, Korea (E-mail: *p_dsjang@cnu.ac.kr*; *sukakim@pony.cnu.ac.kr*)

**Korea Atomic Energy Research Institute, P.O.Box 105, Yuseong, Daejeon 305-353, Korea (E-mail: *shjung3@kaeri.re.kr*)

Abstract To make an indepth diagnosis of a full-scale rectangular secondary clarifier, an experimental and numerical study has been performed in a wastewater treatment facility. Calculation results by the numerical model with the adoption of the SIMPLE algorithm of Patankar are validated with radiotracer experiments. Emphasis is given to the prediction of residence time distribution (RTD) curves. The predicted RTD profiles are in good agreement with the experimental RTD curves at the upstream and center sections except for the withdrawal zone of the complex effluent weir structure. The simulation results predict successfully the well-known flow characteristics of each stage such as the waterfall phenomenon at the front of the clarifier, the bottom density current and the surface return flow in the settling zone, and the upward flow in the exit zone. The detailed effects of density current are thoroughly investigated in terms of high SS loading and temperature difference between influent and ambient fluid. The program developed in this study shows the high potential to assist in the design and determination of optimal operating conditions to improve effluent quality in a full-scale secondary clarifier.

Keywords Density current; density waterfall; residence time distribution; SS; temperature

Water Science & Technology **Vol 54 No 8 pp 83–92** © IWA Publishing 2006

Introduction

Nowadays, the wastewater treatment plant (WWTP) is the one of the significant facilities inevitably required for the conservation of water quality due to the rapid industrialization in Korea. Since the end of 2003, 242 facilities have been operated nationwide (Korea Ministry of the Environment, 2004). The installation plan is scheduled to handle about 80% clarification of sewage generated from the municipal regions. However, most of the WWTPs are over-designed excessively large and further not operated effectively according to the recent statistics of the Korea Ministry of Environment. It is time to evaluate seriously the performance of the WWTP process because of the cost penalty increase for sewage treatment.

The activated sludge process is the widely used form of biological wastewater treatment. Activated sludge has a two-step process related with the biological oxidation and the solids separation. Following the oxidation step, mixed liquor suspended solids (MLSS) from mixed liquor is separated by gravity in a secondary clarifier, which is a common and extensively used application process in WWTP. A portion of the settled biological solids in the clarifier is returned to the aeration tank to maintain an appropriate MLSS concentration. The role of clarification is very important because the effluent quality is directly affected by the separation of the biological solids. Thus, improvement of solid separation in a secondary clarifier will have a great impact on effluent quality, considering the more and more stringent effluent quality standard.

doi: 10.2166/wst.2006.857

Design of clarifiers is mainly based on the parameter of the surface overflow rate (Q/A_c, where Q is the flow rate and A_c is the clarifier cross-sectional area) of the tank. This design variable assumes the uniform plug flow through the tank. Most commonly used design criteria incorporate this relatively simple concept. However, the feature of many full-scale sedimentation tanks does not follow the ideal flow behavior because suspended solids removal in a clarifier is not only a function of overflow rate but also other variables such as density flow, turbulence and multi-dimensional features of flow, etc.

In more detail, the degree of non-uniformity is known as a complex function of the characteristics of the SS (particle size, density, settling velocity, and concentration), the flow field (inlet flow velocity, flow rate, and turbulence intensity), the geometrical configuration of a clarifier and meteorological conditions (McCorquodale and Zhou, 1993; Stamou, 1995). In order to assist in advanced design for sedimentation tanks the effect of the variables mentioned above on the hydraulics of tank flow must be carefully evaluated.

The causes of density currents formed in a clarifier have been still debated in a lively fashion due to the complicated flow pattern. Therefore, residence time distribution (RTD) curves were measured with the application of a radiotracer in order to elucidate the internal flow phenomena in a full-scale secondary clarifier in WWTP. This real time RTD curve can provide various important hydrodynamic parameters but it is not enough to visualize and resolve the detailed flow pattern inside the system. For that reason numerical modeling is performed to figure out the flow pattern and the distribution of SS concentration. The special emphasis of this study is given mainly to analyze the fundamental mechanisms of flow caused by density current in a secondary clarifier with high SS loading.

Experiments

Experiments were carried out in the full-scale rectangular clarifier with a surface area of 120 m^2 and a depth of 3.38 m at Suyoung wastewater treatment plant in Busan, Korea.

RTD was measured by making use of I-131 (8.2 mCi as liquid phase) as a tracer. I-131 (8.04 days) is routinely produced from HANARO, the research reactor in Korea Atomic Energy Research Institute (KAERI), in order to supply domestic hospitals for medical purposes. It may have too long a half-life for this application but it is advantageous in that I-131 is in anionic form in NaI solution and it does not need to be processed any further to make it stable in the water and easy to handle due to relatively low gamma energy.

A radiation detector was developed for practical application in the field because the most popular scintillation detector (NaI) required a heavy lead shield to eliminate background radiation from the surrounding environment. The radiation absorbed into detectors is converted into the scintillation light and the light is amplified by a photo-multiplier tube. Each detector is coupled with a rate meter, which counts the number of pulses generated by a detector and transmits the result to a computer for data recording. The result is converted into a RTD by background subtraction, possible half-life correction and normalization.

Detection was performed at 20 points in the full-scale clarifier, including the inlet and outlet opening. The tracer detection was measured far away from the centreline because the scrapper circulated the whole clarifier to remove scum on top and settling solids on the bottom. Figure 1 shows the schematic of a full scale secondary clarifier and radiotracer detection points for measurements.

Table 1 shows the flow rate introduced into clarifiers during the experiment. The flow rate was fluctuated as time and the average theoretical velocity was calculated as 0.0023 m/sec, the value of which was used to evaluate the strength of density currents.

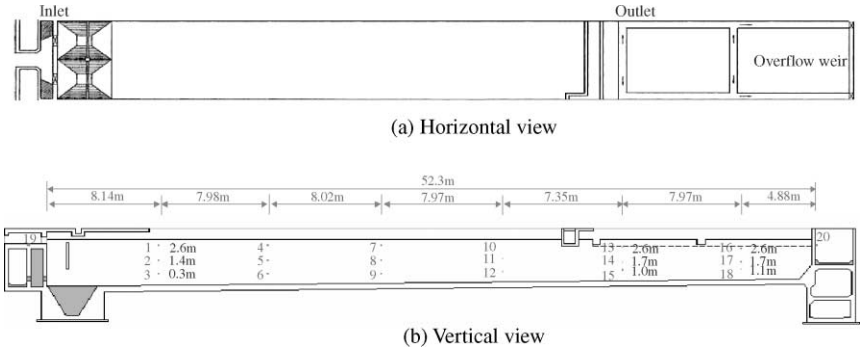

Figure 1 The location of the detector for RTD study in the secondary clarifier

In the field the average MLSS and effluent SS concentrations are respectively about 1,300 mg/L and 5 mg/L.

The temperature between the tank inlet and outlet was measured together with the on-site atmosphere temperature because surface heat transfer would become significant by the effects of solar radiation. During the experiment, solar radiation on the water surface induced temperature increases of 0.5–1.0 °C between the tank inlet and outlet. Solar radiation in summer can eventually produce the temperature increase inside the clarifier, which causes the density current and likewise SS loadings.

Numerical method

Governing equation and solution

The flow patterns for density-stratified fluids in a secondary clarifier are usually different from those simple fluid flows of plug type with uniform density. Even if the relative importance of inertial and gravity forces in the clarifier can be simply characterized in terms of the inlet momentum and buoyancy flux defined by the Froude number (Fr), a computer model for the resolution of complex stratified flow requires a set of conservation equations for continuity and momentum, turbulent kinetic energy k, dissipation of turbulence energy ε and solids concentration (Patankar, 1980). These can be expressed as

$$\frac{\partial(\rho\phi)}{\partial t} + \frac{\partial}{\partial x_j}(\rho u_j \phi) = \frac{\partial}{\partial x_j}\left(\Gamma_\phi \frac{\partial \phi}{\partial x_j}\right) + S_\phi \tag{1}$$

where ϕ denotes general dependent variables expressed as a physical quantity per unit mass. Further, u, v, ρ, Γ_ϕ and S_φ stand for x, y velocity components, density, turbulent diffusion coefficient and source term corresponding to ϕ, respectively.

Table 1 Influent flow rate during experiment

Date	Hour	Flow rate to 36 clarifiers (m^3/3 hrs)	Avg. theoretical velocity (m/s)
1st day	15:00–18:00	23,000	0.002329
	18:00–21:00	26,600	0.002694
	21:00–24:00	28,100	0.002846
2nd day	00:00–03:00	21,400	0.002167
	03:00–06:00	17,500	0.001772
	06:00–09:00	16,100	0.001631
	09:00–11:00	23,300	0.002360
Avg. theoretical velocity* (m/s)		0.002257	

*Average theoretical flow through velocity, $U = Q / WD$

The concentration equation for suspended solid is

$$\frac{\partial C}{\partial t} + u\frac{\partial C_i}{\partial x} + v\frac{\partial C_i}{\partial y} = \frac{\partial}{\partial x}\left(\nu_{sx}\frac{\partial C_i}{\partial x}\right) + \frac{\partial}{\partial y}\left(\nu_{sy}\frac{\partial C_i}{\partial y} + V_s C_i\right) \tag{2}$$

in which ν_{sx} and ν_{sy} are eddy diffusivity of suspended solids in the x- and y-direction; and V_s is particle settling velocity. The eddy viscosity is calculated from the standard k-ϵ turbulence model which relates to the turbulence kinetic energy of k and the turbulence dissipation rate of ε (Orszag, 1993). It has been widely used for many industrially relevant flows.

The SIMPLEC (semi-implicit method for pressure-link consistent equations) algorithm, with a power-law difference scheme presented by Patankar, was applied for the pressure-linked momentum equation (Patankar, 1980). A system of discretized linear equations as shown in Eqn (3) was solved iteratively due to the nonlinear feature of the implicit equation.

$$a_p\phi_p = a_E\phi_E + a_W\phi_W + a_N\phi_N + a_S\phi_S + b \tag{3}$$

where a_E, a_W, a_N, a_S, and a_P are coefficients of east, west, north, south and main grid nodes.

Local density

The local fluid density is related empirically to the local values of temperature and sediment concentration given by

$$\rho = \rho_T + \Delta\rho_S \tag{4}$$

where ρ_T = density as function of temperature, kg/m^3

$\Delta\rho_S$ = density increase by suspended solids, kg/m^3

An empirical equation of density proposed by Gill (1982) was used to incorporate the temperature effect on density. For density-driven flows, the increase of local fluid density is related to the local values of sediment concentration by

$$\Delta\rho_s = C_s\left(S^s_{1-}\right) \times 10^{-3} \tag{5}$$

where C = solid concentration and S_s = the specific gravity of the solid particles, 1.3 (Larsen, 1977; Tchobanoglous and Burton, 1991).

Settling model

A number of empirical formulas have been proposed to describe the relationship between solid concentration and solid settling velocity (Mazzolani *et al.*, 1998). For low SS concentration, settling velocity may be calculated with a discrete settling model (DSM). The settling velocity of particles is dependent on particle size, showing that the larger particle shows up the higher settling velocity. From the photographic measurements, Li and Gancsarczyk (1987) presented the following settling velocity.

$$V_s = 0.35 + 1.77D_i \tag{6}$$

where D_i = cross sectional diameter of SS (in the range of 0.05–1.4 mm).

In this study, DSM was applied to the four groups of particle size for the calculation of settling velocity because DSM could estimate outflow SS concentration more correctly than any other models proposed for a secondary clarifier (Takacs *et al.*, 1991; Kim, 2005; Kim *et al.*, 2005).

Heat flux model

The net surface heat flux was computed by the following Eqn (7) from Ryan *et al.* (1974).

$$\phi_n = 0.94\varphi_{sc}(1-0.65C^2)+5.15\times10^{-13}(T_a+273)^6(1+0.17C^2) - 5.51\times10^{-8}(T_s+273)^4 \quad -[2.7(T_{v,s}-T_{v,a})^{1/3} +3.2W_2](e_s-e_a)\left[1+0.61\frac{T_s-T_a}{e_s-e_a}\right] \tag{7}$$

where φ_{sc} = clear sky solar radiation, W/m^2

T_a = air temperature, °C

T_s = surface temperature, °C

e_s = saturated vapor pressure at water surface temperature, mbar

e_a = vapor pressure of the air, mbar

C = cloud cover fraction from 0 to 1

W_2 = wind speed, m/s

$T_{v,s}$, $T_{v,a}$ = virtual surface and air temperatures, respectively, K

The equilibrium temperature, that was, the theoretical temperature that the water body would reach at steady state, was computed by solving for T_s, in the above equation when φ_n was set equal to zero.

Boundary condition

A uniform, parallel inlet flow was imposed with horizontal velocity of u_0 and vertical velocity, $v = 0$. The turbulence energy level was assumed with specified values of $k = 0.03u_0^2$ and $\varepsilon = C_\mu^{3/4}(k^{3/2}/l_m)$. The inlet SS loading was assumed to be in a well mixed state with dimensionless concentration unit. The water surface was modelled as a symmetric plane where the vertical velocity v and the normal gradients of velocity component u and k were set to zero. For ϵ and concentration C, empirical boundary conditions were used (Imam *et al.*, 1983). The effluent outlet is in the top cells at the end of the tank. Outlet boundary values were computed from outlet grid points by satisfying the overall mass continuity. The clarifier bottom was treated as a perfect-absorbing boundary, where particles might not be resuspended by the fluid flow. At the rigid walls, the wall function approach was applied for the flow parameters, while for the concentration a zero gradient condition was used (Launder and Spalding, 1972). Near the wall k and ϵ could be calculated from the assumption of local equilibrium conditions. Some simplification had to be accepted here with the application of the 2-D model because the longitudinal effluent weirs had 3-D structures.

Results and discussion

Model validation

Figure 2 shows the measured and calculated RTD profiles, where solid and dotted lines represent the experimental and predicted RTD curves, respectively. Channel number (CH) specifies the detection location of the radiotracer along the horizontal flow direction with three different depths as shown in Figure 1.

In the inlet zone, RTDs at CH1 and CH4 show a trend of slow decrease in concentration due to the surface return flow, while the RTDs at CH3 and CH6 rapidly decrease in a quasi-exponential fashion by the existence of strong bottom density currents. In the settling zone, RTD profiles show rather smooth curves like left-handed Gaussian profiles, where rapid bottom density current gradually decreases and thereby SS is favourable to settle down. In the withdrawal zone, the initial arrival time of tracer is delayed compared

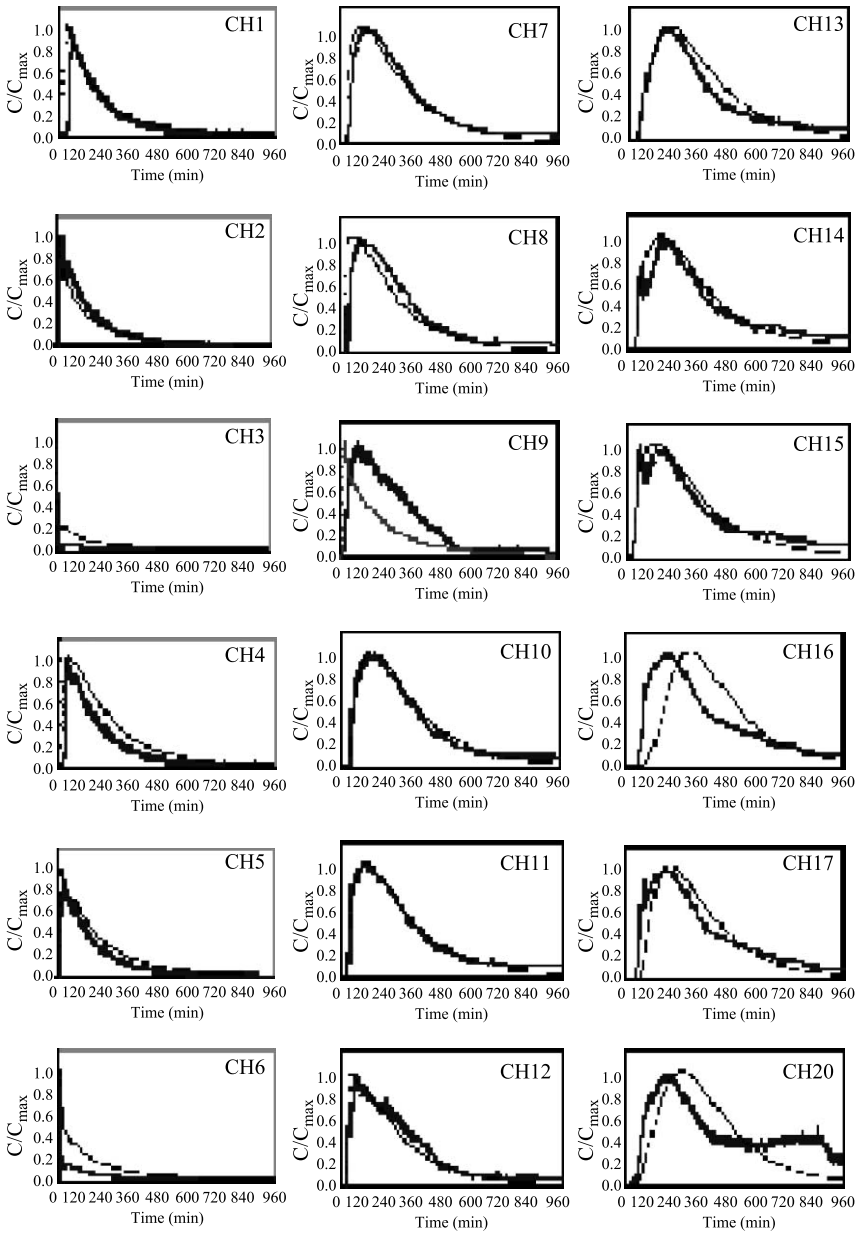

Figure 2 Model validation from RTD comparison with experiment

to other RTDs. Especially in CH16 and CH17, a minor difference between prediction and measurement is noted in RTDs. However, the greater the depth, the more this difference is reduced by the decrease of the effect of top effluent weirs. CH20 is located in the outlet of the clarifier in which the RTD curve represents the retention time of flow. Maximum concentration time of the predicted CH20 appears about 80 minutes longer than that of the experimental RTD. This is because the overflow from four-side weir boards is combined and flows to the exit location. In conclusion, the predicted RTD curves were in good agreement with the experimental RTD curves at the upstream and the middle stream sections except for the location of the discharged weirs.

Density effect by suspended solids

Figure 3 shows the comparison of the flow field due to density effect caused by the SS inlet loading. As shown in Figure 3(a) of neutral density case, the influent flow is deflected downward after impinging on the baffle. The following downward current impinges on the tank bottom below the baffle and then goes along the clarifier bottom and forms a visible recirculation zone near the end wall. In neutral density conditions, plug-type, uniform flow occurs except in the neighborhood of baffle.

Considering the density effect on the flow field as shown in Figure 3(b), the horizontal inlet jet does not reach and strike the inlet baffle, but rather plunges downward to the tank bottom as a density waterfall due to the low densimetric Fr. Under the submerged lip of the baffle, a counter-flow re-entered the inlet zone to provide the entrainment of fluid by the density waterfall. And then the flow forms a forward bottom current over the settling zone and goes upward in the withdrawal zone. The strength of the bottom density current, the upward flow in the withdrawal zone, and the recirculation are increased with a decreasing inlet velocity and higher SS inlet loading (say, low Fr). Therefore, the calculation result shows clearly that SS inlet loading affects significantly the flow pattern in the clarifier.

Density effect by temperature

Both influent and ambient temperatures affecting the flow pattern in the tank were selectively evaluated except for SS loading. Density currents induced by temperature differentials were often found in a primary clarifier with relatively low SS loading.

Figure 4(a) shows the flow condition under the effect of surface cooling in winter. In Figure 4(a), an influent temperature of 2 °C above the ambient temperature caused a strong buoyant flow and significant short-circuiting due to the low hydraulic loading and the large size of the clarifier. A strong forward surface current and the recirculating bottom flow behind the baffle and near the end wall were found in Figure 4(a). On the other hand Figure 4(b) considered the positive heat flux by daytime solar radiation on a

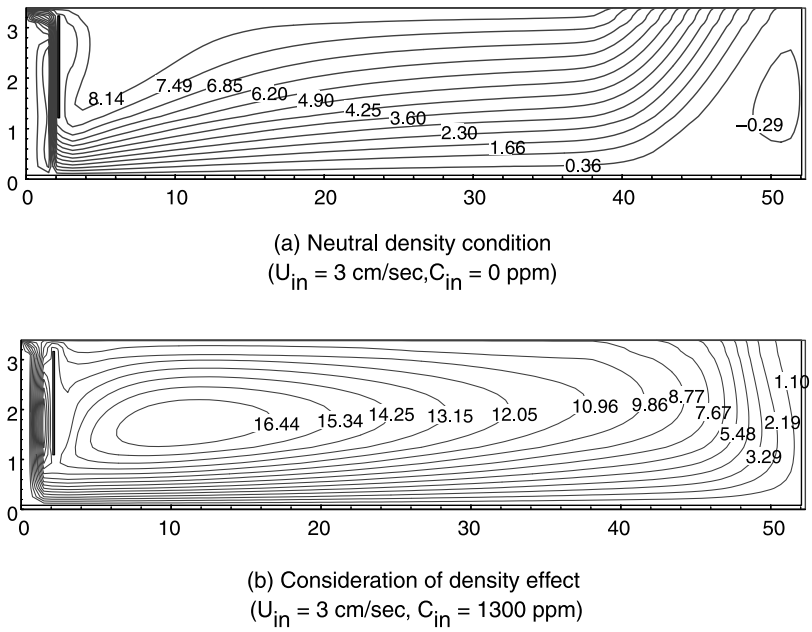

(a) Neutral density condition
(U_{in} = 3 cm/sec, C_{in} = 0 ppm)

(b) Consideration of density effect
(U_{in} = 3 cm/sec, C_{in} = 1300 ppm)

Figure 3 Flow characteristics of a secondary clarifier

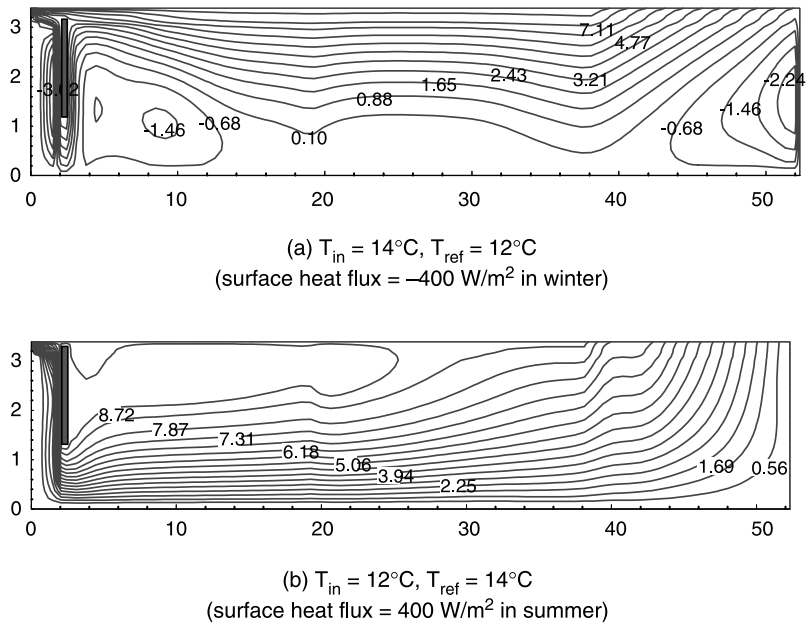

Figure 4 Density currents induced by temperature differences

bright summer day. Cold influent that was 2 °C lower than the ambient temperature created a cascading flow, bottom density current, and surface return flow, which is comparable with the flow pattern by SS loading presented in Figure 4(b).

Behavior of radiotracer

After the flow with SS loading was reached at steady state, radioisotope in aqua-phase was injected at the end of aeration tank as a type of impulse. Thus two component mixtures of tracer and water were modelled to simulate the experiment.

Figure 5 shows the overall spatial distribution of radiotracer concentration with the elapsed time. Tracer forms a high concentration in the bottom of the clarifier due to the strong density current and flows toward the exit along the bottom current as time passes

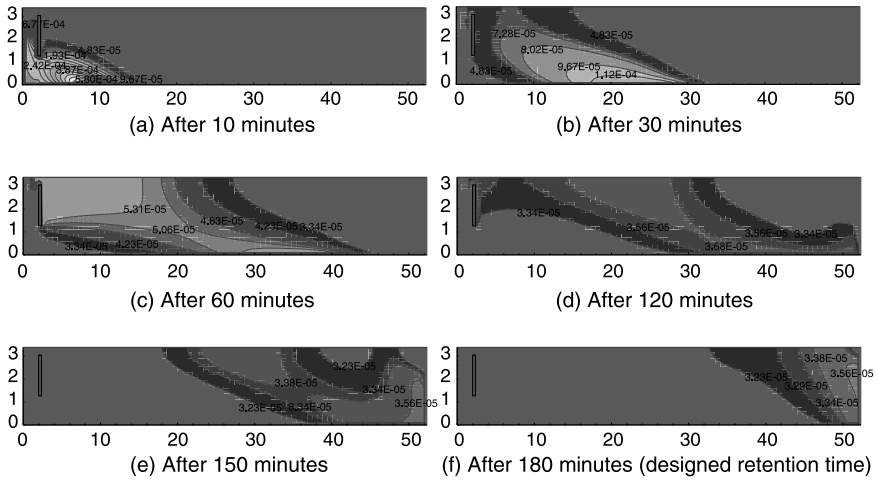

Figure 5 Radiotracer distributions with elapsed time

as shown in Figure 5(a) and (b). In Figure 5(c) and (d), radiotracer shows relatively high concentration behind the inlet baffle by the surface return flow and also the high concentration slowly disappears in the bottom of clarifier. When the radiotracer reaches the withdrawal zone as presented in Figure 5(e) and (f), it diffuses upward and discharges into the effluent weirs. It is expected that lots of tracer leaves is the clarifier approximately after 3 hours, which is in good agreement with the value of the designed residence time. Based on the simulated behaviour of radiotracer, it is determined that the tracer will be detected earlier in the bottom region with higher concentration than any other locationer due to the effect of strong bottom density current.

Conclusions

Based on this study, several useful conclusions can be drawn: numerical simulation predicted successfully the measured RTD curves of radioactive tracer. In detail, the simulated RTD profiles were in good agreement with the experimental RTD curves especially at the upstream and the middle-stream sections but a minor difference was observed at the location of discharge weirs with complex geometry.

This study has shown that clarifier performance is strongly related to hydraulic performance such as density current. For example, injected radiotracer as a pulse type appears to move along the bottom line of the clarifier because of the strong density bottom current. The arrival time of tracer is earlier in the bottom but is delayed on top by the surface return flow. Most tracer leaves out of the clarifier after 3 hours, which is quite a similar value to the designed residence time. The model predicted the well-known flow characteristics in a clarifier such as the waterfall phenomenon at the front end of the clarifier, the strong bottom density current and surface return flow in the settling zone, and the upward flow in the withdrawal zone. In general, it is believed that the numerical model is considered as a viable tool for the proper design and determination of optimal operating conditions of a full-scale clarifier.

References

Gill, A.E. (1982). *Atmosphere-Ocean Dynamics*. Academic Press, New York.

Imam, E., McCorquodale, J.A. and Bewtra, J.K. (1983). Numerical modelling of sedimentation tanks. *Journal of Hydraulic Engineering, ASCE*, **109**(12), 1740–1754.

Kim, H.S. (2005). Numerical modeling of SS separation, thermal drying and incineration pollutant abatement in a sludge and wastes related combined system. Ph. D. thesis, Department of Environmental Engineering, Chungnam National University, Republic of Korea.

Kim, H.S., Shin, M.S., Jang, D.S., Jung, S.H. and Jin, J.H. (2005). Study of flow characteristics in a secondary clarifier by numerical simulation and radioisotope tracer technique. *Applied Radiation and Isotope*, **63**, 519–526.

Korea Ministry of the Environment (2004). Operation trend of sewage treatment plant. http://www.me.go.kr (accessed 10 December 2004).

Larsen, P. (1977). *On the Hydraulics of Rectangular Settling Basins: Experimental and Theoretical Studies*, Department of Water Resources Engineering, Lund Institute of Technology, University of Lund, Lund, SwedenReport No.1001.

Launder, B.E. and Spalding, D.B. (1972). *Mathematical Models of Turbulence*. Academic Press, New York, USA.

Li, D.H. and Gancsarczyk, J.J. (1987). Stroboscopic determination of settling velocity, size and porosity of activated sludge flocs. *Water Research*, **21**(3), 257–262.

Mazzolani, G., Pirozzi, F. and d'Antonoi, G. (1998). A generalized settling approach in the numerical modeling of sedimentation tanks. *Water Science and Technology*, **38**(3), 95–102.

McCorquodale, J.A. and Zhou, S. (1993). Effect of hydraulic and solids loading on clarifier performance. *Journal of Hydraulic Research*, **31**(4), 461–478.

Orszag, S. (1993). Introduction to the renormalization group and turbulence modeling. Guest lecture for users' meeting in Fluent Inc., SRN 713, pp. 1–11.

Patankar, S.V. (1980). *Numerical Heat Transfer and Fluid Flow*. McGraw-Hill Company, Hemisphere Publishing Corporation, USA.

Ryan, P.J., Harleman, D.R.F. and Stolzenbach, K.D. (1974). Surface heat loss from cooling ponds. *Water Resource Research*, **10**, 930.

Stamou, A.I. (1995). *Modelling of Settling Tanks – a critical review*. 3rd International Conference, Water Pollution 95, Porto Carras, Greece.

Takacs, I., Patry, G.G. and Nolasco, D. (1991). A dynamic model of the clarification – thickening process. *Water Research*, **25**(10), 1263–1271.

Tchobanoglous, G. and Burton, F.L. (1991). *Wastewater Engineering*. 3rd edn, McGraw-Hill Publishing Co., New York, USA.